THE JOURNAL OF BIOLOGICAL CHEMISTRY VOL. 288, NO. 27, pp. 19805–19815, July 5, 2013

Liver Fatty Acid-binding Protein Binds Monoacylglycerol *in Vitro* and in Mouse Liver Cytosol*

Received for publication, April 1, 2013, and in revised form, May 4, 2013 Published, JBC Papers in Press, May 8, 2013, DOI 10.1074/jbc.M113.473579

William S. Lagakos[‡1,2], Xudong Guan[§1,3], Shiu-Ying Ho[‡1], Luciana Rodriguez Sawicki[¶], Betina Corsico[¶], Sarala Kodukula[‡], Kaeko Murota[‖], Ruth E. Stark[§], and Judith Storch[‡4]**

*From the [‡]Department of Nutritional Sciences and **Rutgers Center for Lipid Research, Rutgers University, New Brunswick, New Jersey 08901, [§]City University of New York Graduate Center and Institute for Macromolecular Assemblies, New York, New York 10031, [¶]Instituto de Investigaciones Bioquímicas de La Plata, Facultad de Ciencias Médicas, Universidad Nacional de La Plata, 1900 La Plata, Argentina, and [‖]Department of Life Science, Faculty of Science and Engineering, Kinki University, Osaka 577-8502, Japan*

Background: The intracellular carrier protein(s) for monoacylglycerols (MGs) is unknown.
Results: Using chromatography and NMR and fluorescence spectroscopy, we show that liver fatty acid-binding protein (LFABP) is a binding protein for MG and promotes rapid MG transfer to membranes.
Conclusion: LFABP binds MG *in vitro* and in liver cytosol.
Significance: LFABP may transport MG, a metabolic intermediate and signaling molecule, in liver and intestinal cytosol.

Liver fatty acid-binding protein (LFABP; FABP1) is expressed both in liver and intestinal mucosa. Mice null for LFABP were recently shown to have altered metabolism of not only fatty acids but also monoacylglycerol, the two major products of dietary triacylglycerol hydrolysis (Lagakos, W. S., Gajda, A. M., Agellon, L., Binas, B., Choi, V., Mandap, B., Russnak, T., Zhou, Y. X., and Storch, J. (2011) *Am. J. Physiol. Gastrointest. Liver Physiol.* 300, G803–G814). Nevertheless, the binding and transport of monoacylglycerol (MG) by LFABP are uncertain, with conflicting reports in the literature as to whether this single chain amphiphile is in fact bound by LFABP. In the present studies, gel filtration chromatography of liver cytosol from LFABP$^{-/-}$ mice shows the absence of the low molecular weight peak of radiolabeled monoolein present in the fractions that contain LFABP in cytosol from wild type mice, indicating that LFABP binds *sn*-2 MG *in vivo*. Furthermore, solution-state NMR spectroscopy demonstrates two molecules of *sn*-2 monoolein bound in the LFABP binding pocket in positions similar to those found for oleate binding. Equilibrium binding affinities are ~2-fold lower for MG compared with fatty acid. Finally, kinetic studies examining the transfer of a fluorescent MG analog show that the rate of transfer of MG is 7-fold faster from LFABP to phospholipid membranes than from membranes to membranes and occurs by an aqueous diffusion mechanism. These results provide strong support for monoacylglycerol as a physiological ligand for LFABP and further suggest that LFABP functions in the efficient intracellular transport of MG.

In the intestine, dietary triacylglycerol digestion generates large quantities of fatty acids (FAs)[5] and *sn*-2 monoacylglycerols (MGs), which are then taken up by absorptive enterocytes and used primarily for triacylglycerol resynthesis in the endoplasmic reticulum (1, 2). In recent years, it has become appreciated that MGs may be important not only as intermediates in TG synthesis and degradation but also for other reasons. In particular, 2-arachidonoylglycerol has attracted much attention as an endogenous cannabinoid receptor ligand (3, 4). In the intestine, 2-arachidonoylglycerol may play a role in regulating motility and incretin hormone secretion among other properties (5–9).

We reported previously that long chain MGs and FAs are taken up into the enterocyte at least in part via a common protein-mediated pathway (10, 11). Once inside the cell, both lipids must move to intracellular organelles for metabolic processing. Liver fatty acid-binding protein (LFABP; FABP1) is expressed abundantly in the small intestinal mucosa as well as in the hepatocyte. Although it is clear that LFABP binds long chain FAs and likely serves as an intracellular FA transport protein (12, 13), the intracellular transport of MG has been little considered. In mice null for LFABP, we recently showed that intestinal MG metabolism is significantly perturbed but that the changes in MG metabolism are not due to changes in expression of genes related to MG and TG metabolism (14). These results suggest an MG trafficking defect in the LFABP$^{-/-}$ mice; however, a

* This work was supported, in whole or in part, by National Institutes of Health Grant DK-38389 (to J. S.) and Grant 2G12 RR03060 from the National Center for Research Resources and Grant 8G12MD007603 from the National Institute on Minority Health and Health Disparities for additional infrastructural support at The City College of New York. This work was also supported by City University of New York Collaborative Grant 80209 (to R. E. S.) and funds from the New Jersey Agricultural Experiment Station (to J. S.).

[1] These authors contributed equally to this work.
[2] Present address: Dept. of Medicine, University of California, San Diego, 9500 Gillman Dr., La Jolla, CA 92093.
[3] Present address: Inst. for Genomic Biology, University of Illinois, 1206 W. Gregory Dr., Urbana-Champaign, IL 61801.
[4] To whom correspondence should be addressed: Dept. of Nutritional Sciences, Rutgers University, 96 Lipman Dr., New Brunswick, NJ 08901. E-mail: storch@aesop.rutgers.edu.

[5] The abbreviations used are: FA, fatty acid; MG, monoacylglycerol; TG, triglyceride; LFABP, liver fatty acid-binding protein; 12AO, 12-(9-anthroyloxy)oleic acid; MG12AO, 12-(9-anthroyloxy)oleoyl-*sn*-1-glycerol; EPC, egg phosphatidylcholine; NBD-PE, *N*-(7-nitro-2,1,3-benzoxadiazol-4-yl)phosphatidylethanolamine; OA, oleic acid; SUV, small unilamellar vesicle; Q, quantum yield(s); FABP, fatty acid-binding protein; IFABP, intestinal fatty acid-binding protein.

controversy exists as to whether LFABP binds MG. Using a fluorescence displacement assay, it was concluded that monoolein does not bind to LFABP (15), whereas other studies showed binding of a fluorescent monoolein analog to LFABP and quenching of the intrinsic tyrosine fluorescence of LFABP by monoolein addition (16), suggesting that MG does bind to LFABP. To understand the basic mechanism of intracellular MG transport as well as the mechanism underlying the effects of LFABP gene ablation on intestinal MG metabolism, it is important to determine unequivocally whether or not monoacylglycerol is a ligand for LFABP.

In the present studies, we used chromatographic analysis of liver cytosol from wild type and LFABP-null mice, equilibrium binding studies, structural perturbation of LFABP monitored by NMR spectroscopy, and transfer kinetics of a fluorescent monoolein analog to demonstrate that MG binds to LFABP both *in vitro* and *in vivo* and can serve to efficiently transfer MG to acceptor membranes. The results resolve the controversy and provide strong support for a role for LFABP as an intracellular MG transport protein.

EXPERIMENTAL PROCEDURES

Materials—Rat LFABP was purified as described previously (17). [^{14}C]Oleic acid ([1-^{14}C]oleic acid; 54 mCi/mmol) was obtained from PerkinElmer Life Sciences. [^{3}H]Monoolein (*sn*-2 [9,10-^{3}H]monoolein; 40–60 Ci/mmol) was from American Radiolabeled Chemicals (St. Louis, MO). Quinine sulfate and antibodies to human albumin were obtained from Sigma-Aldrich. U-^{15}N-enriched recombinant rat LFABP was expressed in *Escherichia coli* in $^{15}NH_4Cl$ minimal medium as described previously (18, 19). Antibodies to purified rat LFABP were generated in rabbits by Affinity Bioreagents (Golden, CO) (14). 12-(9-Anthroyloxy)oleic acid (12AO) was from Molecular Probes, Inc. (Eugene, OR). Unlabeled sodium oleate and *sn*-1 monoolein were obtained from Sigma. Unlabeled *sn*-2 monoolein was obtained from Doosan Serdary Research Laboratories (Toronto, Canada). The fluorescent MG analog 12-(9-anthroyloxy)oleoyl-*sn*-1-glycerol (MG12AO) was synthesized by condensation of 12AO with glycerol 1,2-isopropylidene ketal (Molecular Probes, Inc.), and the structure was verified by NMR spectroscopy as reported previously (20). Egg phosphatidylcholine (EPC) and *N*-(7-nitro-2,1,3-benzoxadiazol-4-yl) phosphatidylethanolamine (NBD-PE) were obtained from Avanti Polar Lipids (Birmingham, AL). All other materials were reagent grade or better.

Animals and Tissue Harvest—Liver tissue was harvested from male C57BL6/J wild type and congenic LFABP$^{-/-}$ mice (14) following perfusion via the inferior vena cava with phosphate-buffered saline, pH 7.4 (PBS) and homogenized with a Potter-Elvehjem homogenizer in PBS with 0.5% protease inhibitor mixture (Sigma 8340) on ice. The homogenate was centrifuged at 600 × *g* for 10 min at 4 °C, and the supernatant was further centrifuged at 105,000 × g for 90 min at 4 °C to obtain a cytosol fraction. Protein concentration was determined by the Bradford method (21).

Cytosolic FA and MG Binding—Cytosolic lipid binding capability was assessed as described by Martin *et al.* (22). In brief, a 1.5 × 30-cm Superdex G75 column was equilibrated with PBS and calibrated with a molecular mass kit (Sigma) including aprotinin (6.5 kDa), cytochrome *c* (12.4 kDa), carbonic anhydrase (29 kDa), and albumin (66 kDa). 10 mg of cytosol protein in 250 μl of PBS was incubated with 5 μCi of [^{14}C]oleate or 5 μCi of [^{3}H]monoolein for 10 min at 25 °C and loaded onto the column. Fractions were eluted with PBS at 1 ml/min, and the protein concentration of the eluent was monitored continuously by spectrophotometry (λ_{abs}, 280 nm). 2-ml fractions were collected on ice. 10-μl aliquots were used for scintillation counting. Fractions were concentrated to 0.5 ml using Amicon centrifugal filter units (10,000 molecular weight cutoff).

Immunoblotting—35 μl of concentrated fractions and 3 μg of purified LFABP were loaded onto 15% polyacrylamide gels and separated by SDS-PAGE. The proteins were transferred to a 0.45-μm nitrocellulose membrane using a Semi-Dry transfer system (Bio-Rad) for 1 h 20 min at 20 V. The membranes were incubated in a 5% nonfat dry milk blocking solution overnight at 4 °C and then washed with two 5-min rinses and one 15-min rinse with wash buffer (0.05 M Tris-HCl, 0.15 M NaCl, 0.1% Tween 20, pH 7.6). Membranes were then incubated with the anti-rat LFABP antibody (14) at 1:5,000 in PBS for 1.5 h at room temperature. Following washing as above, the membranes were incubated with the secondary antibody (rat anti-rabbit IgG; 1:10,000) for 1 h and then visualized by chemiluminescence (ECL reagent, GE Healthcare).

Ligand Binding Affinities—The binding affinities of oleate and monoolein to purified LFABP were estimated using the Lipidex 1000 assay as described by Glatz and Veerkamp (23). Briefly, 10 mM Tris-HCl buffer, pH 8.0 was used to dilute oleic acid, monooleoylglycerol, and LFABP stock solutions. [^{14}C]Oleic acid dilutions from 1 to 10 μM were freshly prepared from an ethanolic stock solution ([1-^{14}C]oleic acid; 54.4 mCi/mmol; 250 μCi in ethanol; PerkinElmer Life Sciences). [^{3}H]Monooleoylglycerol dilutions from 1 to 10 μM were freshly prepared by adding 0.5μCi of [^{3}H]monooleoylglycerol (2-monooleoyl[9,10-^{3}H]glycerol; 60 Ci/mmol; 250 μCi in acetonitrile; American Radiolabeled Chemicals) to 4 ml of a 10 μM solution of 2-monooleoylglycerol (C18:1, *cis*-9, Sigma). For the binding assay, 150 μl of buffer, 50 μl of LFABP solution (2.72 μM), and 50 μl of ligand solution were mixed in this order in a 1.5-ml Eppendorf polypropylene reaction vial. After incubation for 15 min at 37 °C, vials were centrifuged for 5 s and placed on ice. From each vial, 50 μl was used for scintillation counting to determine the ligand concentration in the aqueous solution. To the remaining 200 μl, 50 μl of continuously stirred ice-cold Lipidex 1000 suspension (Sigma) was added and mixed three to four times on a Vortex mixer during a 30-min incubation period at 0 °C. Finally, the vials were centrifuged (2 min at 10,000 × *g* at 4 °C), and 100 μl of supernatant was transferred to a scintillation vial and used to quantify the amount of bound ligand. Radioactivity was measured with a PerkinElmer Wallace 1409 DSA liquid scintillation counter (PerkinElmer Life Sciences). Blank values obtained for each ligand dilution by measuring the radioactivity of incubations in which 50 μl of buffer without LFABP was added were subtracted. Data were analyzed using the Hill equation $(x/(n - x)) = c \log[\text{ligand}]_i + \log K'$ where x is ligand bound/total LFABP, n is the number of binding sites, and c is the Hill coefficient.

Preparation of NMR Samples—A 0.40 mM solution of U-^{15}N-enriched apo-LFABP was prepared in 10 mM NaH_2PO_4, 250 mM NaCl, 5 μM EDTA, 0.02% NaN_3, and 5% D_2O at pH 6.0. For titration of LFABP with oleic acid (OA), 1.8-μl aliquots of 100 mM sodium oleate were added successively to 579 μl of the apoprotein, corresponding to complexes of [^{15}N]LFABP with protein-to-ligand molar ratios of 1:0.4, 1:0.8, 1:1.2, 1:1.6, 1:2.0, and 1:3.0, respectively, as used in a prior set of experiments (24). For titration of LFABP with monoolein, a stock solution containing 17.1 μg of the monoglyceride in hexanes was dried with a stream of nitrogen for 30 min in a small glass vial. Then 600 μl of 0.4 mM LFABP was added to obtain a 1:0.2 protein-ligand complex. This solution was added to another 17.1 μg of MG film in a different glass vial to form a 1:0.4 protein-ligand complex and so on to obtain molar ratios of 1:0.6, 1:0.8, 1:1.0, 1:1.2, 1: 1.4, 1: 1.6, 1:1.8, and 1:2.0.

NMR Experiments and Analysis—The NMR spectra were acquired on a VNMRS 600 Varian/Agilent spectrometer equipped with a Nalorac ^{1}H-optimized four-nucleus gradient probe and operating at 599.761 MHz. Two-dimensional ^{1}H-^{15}N heteronuclear single quantum correlation NMR spectroscopy data (25) were recorded with 512 × 128 complex points and 16 transients; measurements were made at 37 °C. The ^{1}H carrier frequency was set at the water peak (referenced to 4.629 ppm at 37 °C), and the ^{15}N carrier frequency was set in the middle of the amide region (119.44 ppm). Chemical shifts were referenced following the guidelines of Wishart and Sykes (26). Two-dimensional data were processed with NMRPipe software (27) and analyzed with NMRViewJ (28).

Assignments for 89.8% of the amino acid residues in the apoprotein were taken from He *et al.* (24). The titrations were monitored by following the chemical shift changes in ^{1}H-^{15}N heteronuclear single quantum correlation spectra of the protein upon addition of OA or MG ligands. Chemical shift perturbations for each backbone cross-peak were calculated with the following equation: $\Delta_{HN\text{-}N} = \{[\delta_{HN}(apo) - \delta_{HN}(complex)]^2 + [(\delta_N(apo) - \delta_N(complex))/6.5]^2\}^{1/2}$ (29).

Vesicle Preparation—Small unilamellar vesicles (SUVs) were prepared from 90 mol % EPC and 10% NBD-PE as described (30). The phospholipid concentration of the vesicles was determined by quantification of inorganic phosphate (31).

Fluorescence Measurements—Fluorescence spectra were obtained with an SLM 8000C fluorescence spectrophotometer. Measurements were carried out at 24 °C in 3 × 3-mm microcuvettes containing ~0.3 ml of sample. Excitation wavelengths were set at 383 nm for 12AO and MG12AO and 352 nm for quinine sulfate. The fluorescence quantum yields (Q) for both probes bound to LFABP as well as to EPC SUVs were determined relative to quinine sulfate in 0.1 N sulfuric acid. Spectra were corrected for lamp and photomultiplier variation with wavelength (32). The value of Q for the quinine sulfate reference was 0.7 (33).

Transfer of 12AO and MG12AO from LFABP to SUVs—The transfer of 12AO and MG12AO from LFABP to acceptor SUVs and analysis of the resulting data were conducted as described previously (34–36). Briefly, LFABP was incubated with 12AO or MG12AO for ~15 min at room temperature. A volume of this donor complex was then mixed with an equal volume of acceptor SUVs containing 10 mol % NBD-PE using an Applied Photophysics SX17MV temperature-controlled stopped flow spectrometer (Applied Photophysics Ltd., UK). The NBD moiety is an energy transfer quencher of the AO fluorescence (34). Because 12AO and MG12AO bound to LFABP are fluorescent, the rate of 12AO or MG12AO transfer from LFABP to quencher-containing SUVs was monitored directly by the decrease in fluorescence intensity over time following mixing. Except where noted, the final transfer assay mixture contained 6 μM LFABP, 1 μM 12AO or MG12AO, and 360 μM acceptor SUVs; transfer was monitored at 24 °C. The standard assay buffer was Tris-buffered saline (40 mM Tris-HCl, 100 mM NaCl, pH 7.4). Tris buffer was used for studies from pH 6 to 9, and acetate buffer was used for studies at pH 5. Software provided with the instrument was used to analyze the transfer curves. The curves for 12AO and MG12AO transfer from LFABP to EPC membranes were best fit by a single exponential function, and the curves for intermembrane transfer were best fit by a double exponential function in agreement with previous work (20, 34). For each experimental condition, 5–10 replicates were done to derive average transfer rates. Results are mean ± S.D. from at least five separate experiments.

RESULTS

Reduced FA and MG Binding in LFABP$^{-/-}$ Liver Cytosol—The elution profiles of [^{14}C]oleate and [^{3}H]monoolein in liver cytosol from wild type and LFABP$^{-/-}$ mice are shown in Fig. 1. In WT cytosol, fractions containing high [^{14}C]oleate (Fig. 1*A*) contained LFABP as shown by immunoblotting (Fig. 1*E*) and in agreement with the results of Martin *et al.* (22). By contrast and again in agreement with Martin *et al.* (22), the [^{14}C]oleate peak is entirely absent from the corresponding fractions from LFABP$^{-/-}$ cytosol (Fig. 1*B*), and immunoblotting showed no LFABP in those fractions as expected (Fig. 1*E*). These results confirm that LFABP is the major binding protein for oleate in liver cytosol. The small radioactivity peaks at higher molecular weight are likely due to albumin, which was not removed by liver perfusion. It is worth noting that in the intact hepatocyte albumin is present in the secretory vesicle system, not as a cytosolic protein.

As shown in Fig. 1*C*, in WT cytosol, [^{3}H]monoolein eluted in fractions shown by immunoblotting to contain LFABP (Fig. 1*F*), and neither the radioactivity peak (Fig. 1*D*) nor LFABP (Fig. 1*F*) was present in the corresponding fractions from LFABP$^{-/-}$ cytosol. In the LFABP$^{-/-}$ cytosol fractionation, a peak of [^{3}H]monoolein was also found in a fraction containing peptides of <6.5-kDa molecular mass. It is likely that in the absence of a binding protein monoacylglycerols form micelles, which elute at a low apparent molecular weight. The slight discordance between the peaks of [^{3}H]monoolein radioactivity and Western blot density could be due to small variations in sample concentration, Western blot transfer, and/or immunodetection. Alternatively, the high specific activity of the [^{3}H]monoolein used, resulting in low levels of added ligand, may mean that the LFABP detected by Western blot represents a combination of LFABP bound to labeled MG plus LFABP bound to endogenous ligand. Overall, the results demonstrate that in the liver LFABP is the major intracellular binding protein for monoacylglycerol.

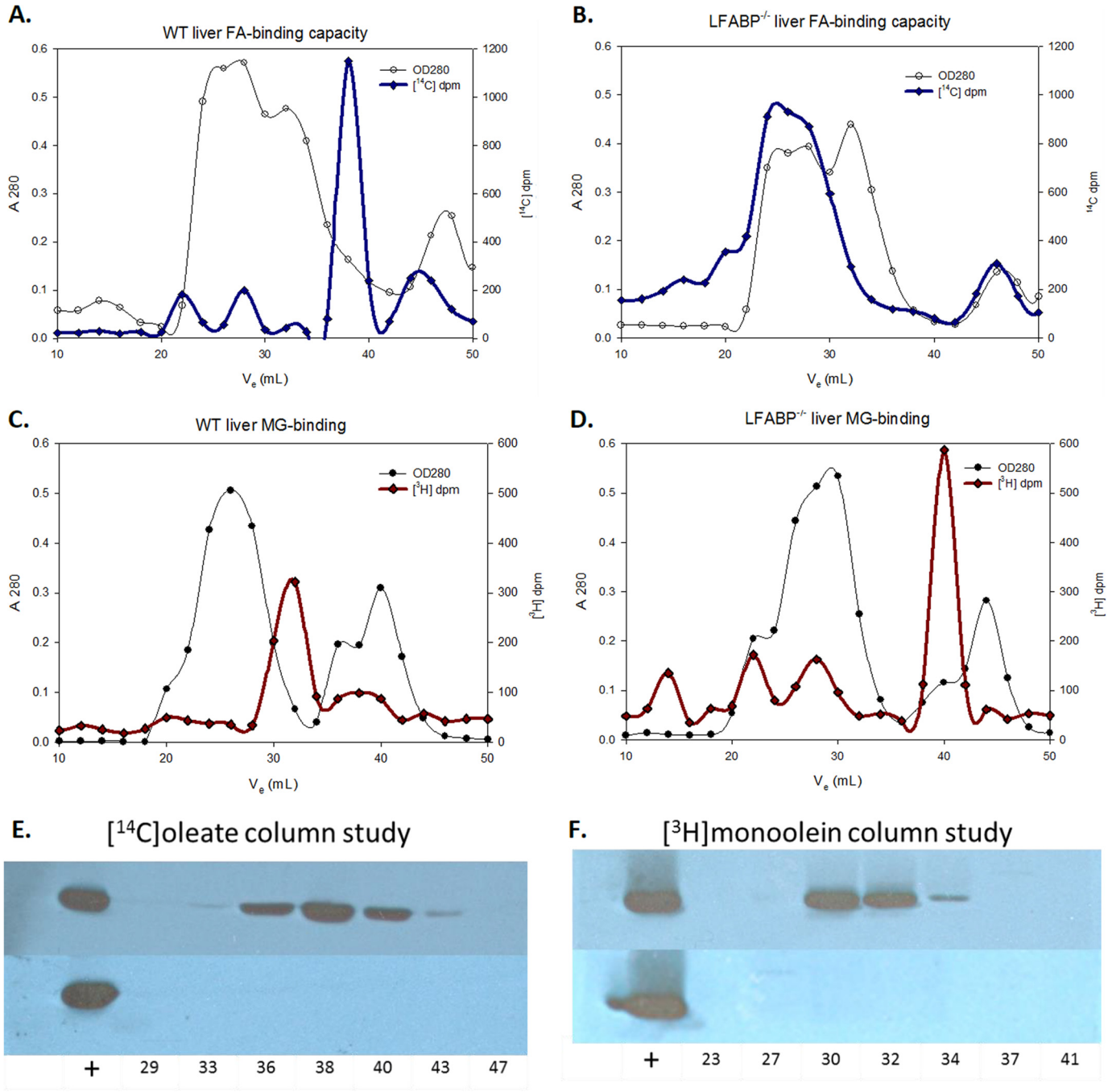

FIGURE 1. **[^{14}C]Oleate and [^{3}H]monoolein retention by WT and LFABP$^{-/-}$ liver cytosol.** Representative chromatograms of 10 mg of WT and LFABP$^{-/-}$ cytosol (A_{280}; *hollow symbols*) and [^{14}C]oleate (*A* and *B*) or [^{3}H]monoolein (*C* and *D*) radioactivity (dpm; *solid symbols*) plotted against elution volume (ml) are shown. Separate columns were packed for the two [^{14}C]oleate and the two [^{3}H]monoolein fractionations. 50 μl of concentrated fraction volume was probed for LFABP in multiple fractions from each of the runs; LFABP immunoblots are shown in *E–H*. The fractions are labeled by their elution volumes, and the *first lane* in each immunoblot is the positive control 3 μg of purified LFABP.

Equilibrium Binding Analysis—Lipidex binding analysis (23) was used to estimate the oleate and monoolein binding affinities for LFABP. Titrations with both ligands appeared sigmoidal with Hill coefficients (the slope of the Hill plot at $\log(x/(n-x)) = 0$) close to 2, suggesting positive binding cooperativity, a result consistent with our previous studies of sequential fatty acid binding to two binding sites (18, 37). The apparent dissociation constants, K', obtained for both ligands using the Hill equation are 34.1 ± 10.4 nM ($n = 5$) for oleate and 63.4 ± 7.8 nM ($n = 6$) for monoolein ($p < 0.005$). Because the LFABP tertiary structures show that the two ligand binding sites are not equivalent, we also approximated the dissociation constants for each site. To obtain a value of K_{d1}, an extrapolation of the curve from high ligand concentrations was performed, and to obtain a value of K_{d2}, an extrapolation of the curve from low ligand concentrations was used. For oleate binding, the K_{d1} and K_{d2} values obtained were 0.8 ± 0.5 and 42.2 ± 10.2 nM, respectively; for monoolein binding, K_{d1} and K_{d2} values were 2.7 ± 1.1 nM ($p < 0.05$ compared with oleate) and 96.7 ± 21.4 nM ($p < 0.001$ compared with oleate), respectively. Representative analyses for each ligand are shown in Fig. 2.

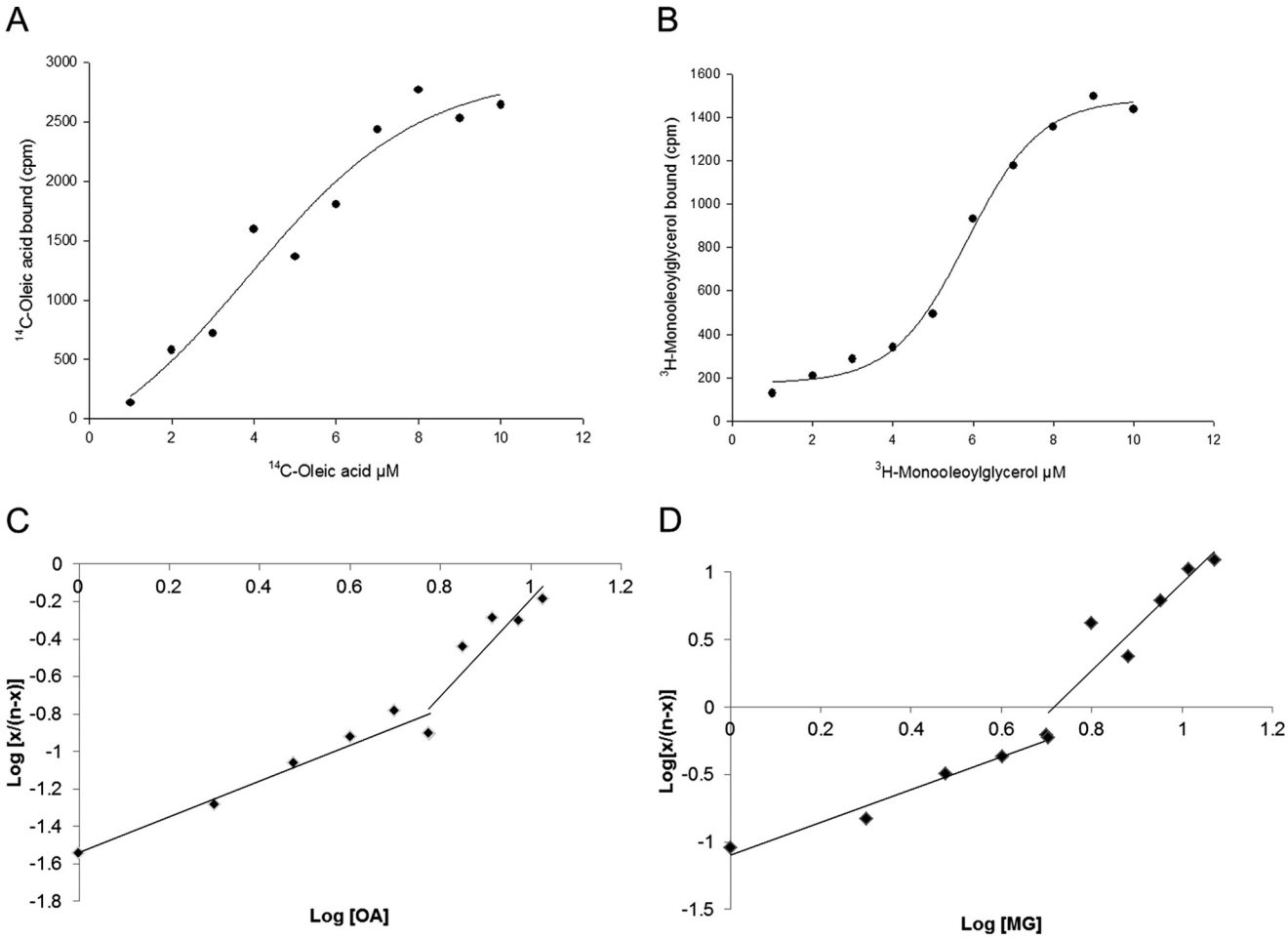

FIGURE 2. **FA and MG binding to LFABP.** The Lipidex assay was used to estimate equilibrium binding affinities as described under "Experimental Procedures." Representative plots of sigmoidal curves of ligand concentration (μM) *versus* ligand bound (cpm) are shown (*A* and *B*). Dissociation constants for each binding site were estimated by extrapolation of the curve from high ligand concentrations (to obtain K_{d1}) and by extrapolation of the curve from low ligand concentrations (for K_{d2}).

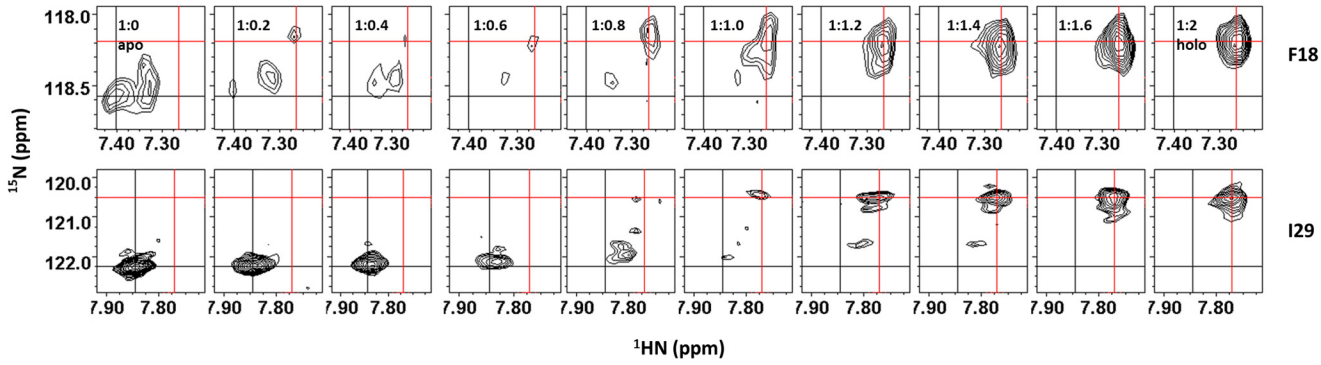

FIGURE 3. **Representative expanded regions of the ^{1}H-^{15}N heteronuclear single quantum correlation NMR contour plots for wild-type LFABP monitored during the ligand titration as the protein-to-MG ratio varies from 1:0 to 1:2.** The chemical shift of residue Phe-18 is perturbed mainly from 0 to 0.8 eq of added MG (*upper panels*), whereas residue Ile-29 is perturbed mainly from 0.8 to 2.0 eq of added MG (*lower panel*). The positions of the apo- and holoprotein forms are indicated by *black* and *red crosshairs*, respectively.

Monoolein Titration of LFABP Monitored by NMR Spectroscopy—The binding of MG (monoolein) to LFABP in a two-step fashion similar to OA (24) was demonstrated by using two-dimensional NMR spectroscopy to monitor titration of the protein with this ligand. Particular protein NH backbone sites exhibited chemical shift perturbations (Δδ) due to changes in magnetic environment associated with ligand binding as shown in the ^{1}H-^{15}N correlation spectra of Fig. 3. Some of the affected sites showed contrasting behavior in terms of whether the environmental perturbation occurred principally at the early titration stages (*e.g.* Phe-18, 0.6–0.8 eq of MG) or at later stages (*e.g.* Ile-29, 1.0–1.2 eq of MG). A perturbation analysis of the full polypeptide chain (summarized graphically in Fig. 4) showed that residues Ser-11, Phe-18, Glu-72, Gly-106, and Lys-121 (at

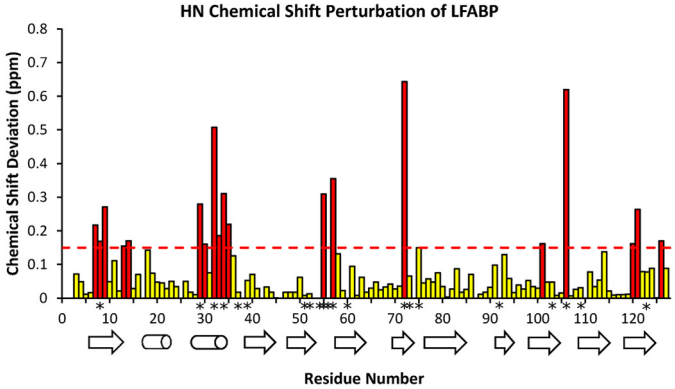

FIGURE 4. **Composite ^{1}H-^{15}N chemical shift perturbation of wild-type LFABP backbone atoms by 2.0 eq of monoolein plotted along the protein sequence and with respect to α-helical and β-strand secondary structural elements.** Perturbations are calculated for instance as Δ(apo − holo) (ppm) = $\{[\delta_{HN}(apo) - \delta_{HN}(complex)]^2 + [(\delta_N(apo) - \delta_N(complex))/6.5]^2\}^{1/2}$ (29). The *dashed line* at 0.15 ppm, set slightly below the mean ± S.D. of perturbations for the pair of protein forms, serves as a guide to identify backbone sites with structurally significant chemical shift changes (highlighted in *red*). Backbone sites that show significant chemical shift perturbations for both MG and OA ligands are designated by *asterisks* (*) along the *residue number axis*.

internal locations within the protein cavity) were affected initially upon ligand addition, whereas Ile-29, Lys-33, Ile-35, and Tyr-120 (at aqueous solution-accessible helical locations near the protein portal) were perturbed predominantly at later stages of MG addition. The broadening of these polypeptide backbone resonances observed during this titration, which was not evident in the analogous OA-LFABP experiments (24), is indicative of two or more differently ligated protein forms with intermediate exchange rates ($k \sim \Delta\delta$).

Monoolein Locations in the LFABP Complex from Solution-state NMR Spectroscopy—The environmentally perturbed LFABP residues listed above were mapped onto the oleate-bound structure derived by solution-state NMR methods (18), forming a roughly contiguous interface that defines the likely locus of monoolein binding sites and argues against an interpretation involving global protein conformational changes (data not shown). Moreover, all residues affected by MG were also perturbed during the analogous OA titration (24), suggesting monoglyceride locations in accord with the structures of the protein-FA complex solved in crystals (38) and in solution (18). Specifically, binding of the first MG or OA ligand altered the magnetic environment of Gly-106, Lys-121, and Glu-72/Thr-73, whereas binding of the second MG or OA ligand affected Ile-29, Lys-33, Ile-35, and Tyr-120. Additionally, the first MG ligand perturbed Ser-11 and Phe-18, an observation that may be attributed to the larger glycerol headgroup as compared with the OA carboxyl and to a partially extended rather than U-shaped conformation for the first ligand (Fig. 5).

Fluorescence Properties of 12AO and MG12AO with LFABP—The fluorescence emission maxima of both LFABP-bound MG12AO and LFABP-bound 12AO were considerably blue-shifted (441 and 438 nm, respectively) with respect to emission of membrane-bound MG12AO (449 nm) and membrane-bound 12AO (451 nm) (Fig. 6). This result suggests a similarly high degree of motional constraint for protein-bound MG12AO and protein-bound 12AO (39). Table 1 shows the fluorescent Q values for 12AO or MG12AO in LFABP com-

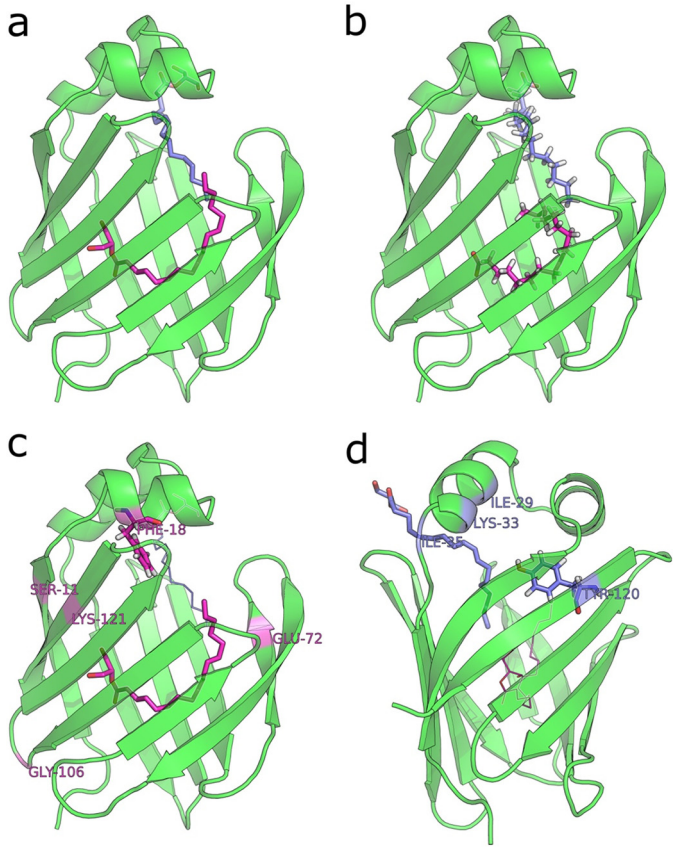

FIGURE 5. **Monoolein and oleate locations within the wild-type LFABP protein cavity.** *a*, monoolein locations consistent with observed chemical shift perturbations upon titration of LFABP with 2 eq of ligand. *b*, oleate locations determined from lowest energy solution structures of the 2:1 complex with LFABP in solution (18). *c*, residues perturbed by the first MG ligand to enter. *d*, residues perturbed by the second MG ligand.

pared with EPC vesicles. The Q for MG12AO in EPC SUVs is lower than that of 12AO in EPC SUVs, suggesting that the AO moiety of MG12AO may penetrate less deeply in EPC SUV membranes than the AO moiety of the 12AO fatty acid analog. The results also show that when bound to LFABP quantum yields for MG12AO and 12AO are virtually identical. Collectively, these results demonstrate that MG12AO and 12AO are bound to LFABP in a similar manner. Both probes appear to experience a highly hydrophobic binding site in which the motion of the fatty acid chain is restricted.

12AO and MG12AO Transfer from LFABP to Small Unilamellar Vesicles—As shown in Fig. 7*A*, the rate of transfer of MG12AO from LFABP to EPC SUVs is very similar to that of 12AO; transfer rates were 0.027 ± 0.002 and 0.028 ± 0.003 s^{-1} for 12AO and MG12AO, respectively. In distinct contrast, the rate of MG12AO transfer from SUV to SUV (0.004 ± 0.001 s^{-1}) is 7-fold slower than that of 12AO (0.029 ± 0.002 s^{-1}) (Fig. 7*B*). In previous studies, it was shown that the transfer of fluorescently labeled FA from LFABP to SUVs occurs via diffusion through the aqueous phase (40, 41). To examine the mechanism of transfer of MG12AO from LFABP to SUVs, the transfer rate was determined for a constant donor LFABP concentration and varying concentrations of acceptor vesicles. As shown in Fig. 8, upon increasing the concentration of SUV acceptors, no change in the transfer rate of either 12AO or MG12AO from

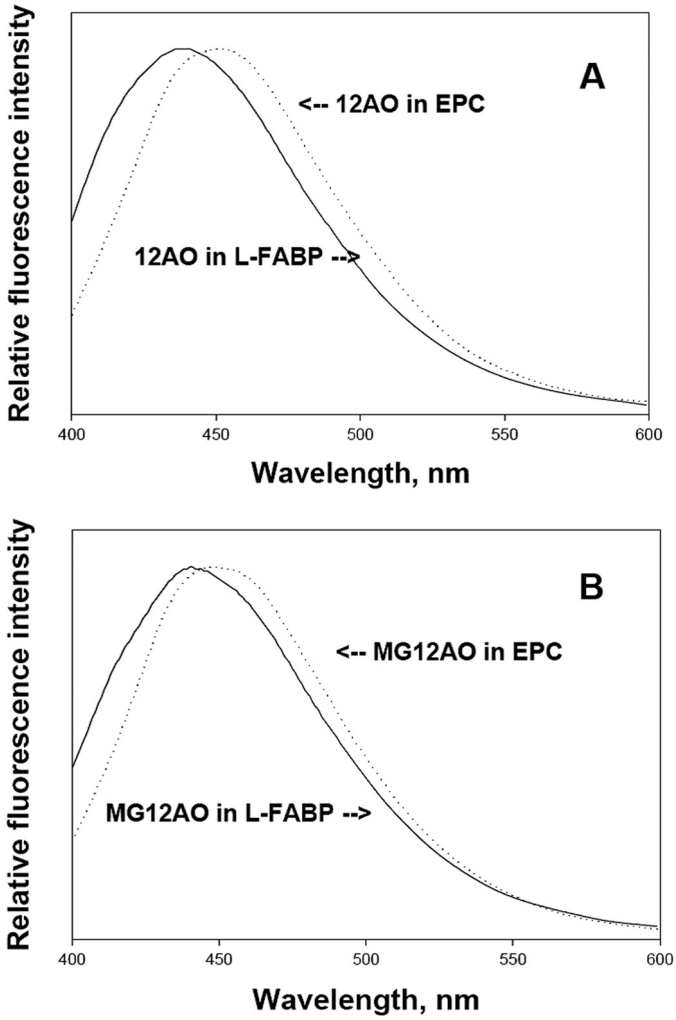

FIGURE 6. **Emission spectra for 1 μM 12AO (*A*) or MG12AO (*B*) bound to 5 μM LFABP (*solid line*) or to 0.1 mM EPC SUVs (*dotted line*) at pH 7.4.** Measurements were carried out at 24 °C. The excitation wavelength was 383 nm.

TABLE 1

Fluorescence Q for 12AO or MG12AO in LFABP or in EPC SUVs

The Q for 12AO and MG12AO was determined relative to quinine sulfate in 0.1 N sulfuric acid. 4 μM ligands were incubated with 80 μM LFABP at room temperature for at least 10 min. 10 μM ligands were incubated with 200 μM EPC SUVs at room temperature for at least 10 min. Results are means ± S.D. from five separate experiments.

	Quantum yield	
	LFABP	EPC
12AO	0.46 ± 0.09	0.51 ± 0.14
MG12AO	0.48 ± 0.17	0.21 ± 0.05

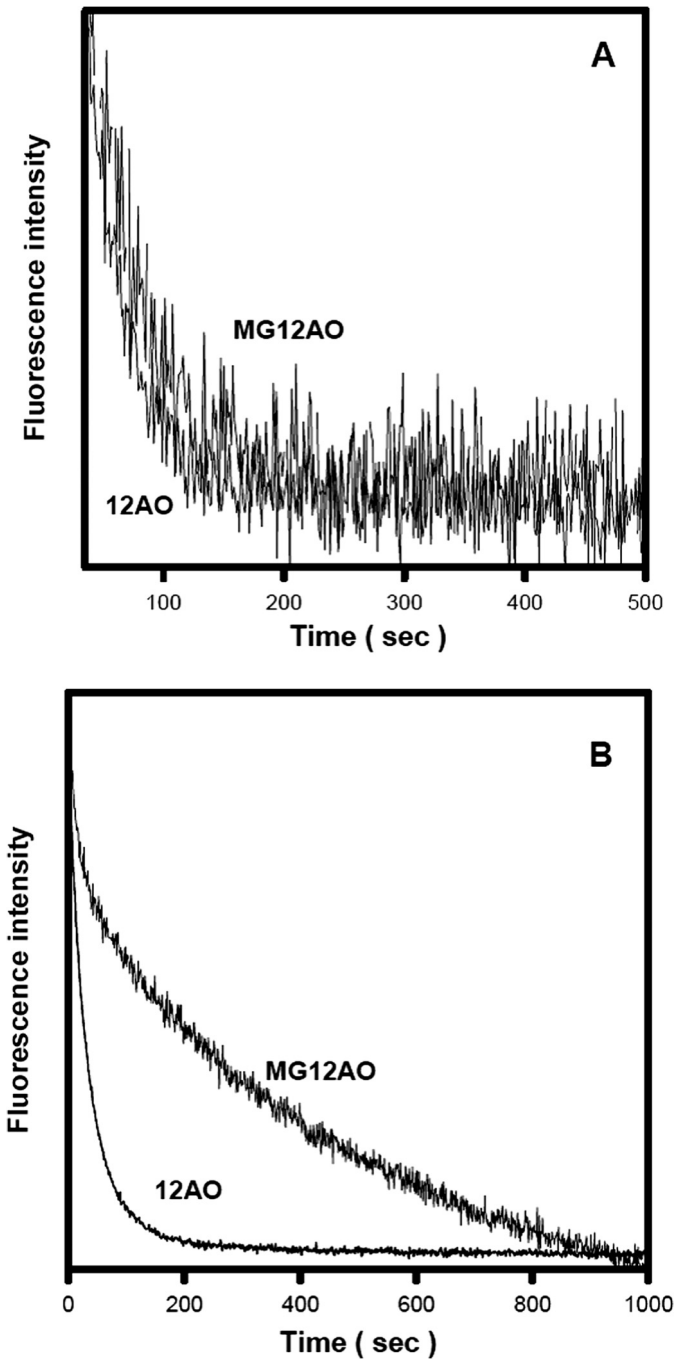

FIGURE 7. **MG12AO and 12AO transfer from LFABP *versus* SUVs.** *A*, the transfer of MG12AO and 12AO from LFABP to SUVs was measured at 24 °C at pH 7.4 as described under "Experimental Procedures." Each time course was normalized to maximum fluorescence intensity. Final concentrations were 1 μM probe with 6 μM LFABP and 0.36 mM 10% NBD-PE, 90% EPC acceptor SUVs. *B*, the transfer of MG12AO and 12AO from SUV to SUV. Conditions were as described in Fig. 3*A*. Final concentrations were 5 μM probe with 0.1 mM donor EPC SUVs and 0.5 mM 10% NBD-PE, 90% EPC acceptor SUVs. Data shown are from one of eight representative experiments.

LFABP to SUVs was observed, suggesting that the transfer of both fatty acid and monoacylglycerol analogs from LFABP to SUVs occurs by a similar aqueous diffusion mechanism.

To further evaluate the influence of aqueous MG solubility on its rate of transfer from LFABP to SUVs, the effect of ionic strength was examined. Increasing the NaCl concentration of the buffer from 0.1 to 2 M caused a logarithmic decrease in the rate of MG12AO transfer from LFABP to SUVs (Fig. 9). The highest NaCl concentration (2 M) decreased the transfer rate by 4-fold compared with physiologic ionic strength. As shown previously, no major alterations in LFABP structure are caused by these NaCl levels (40). This result is virtually identical to what we found previously for 12AO transfer from LFABP to SUVs (40), further suggesting that aqueous solubility directly influences the MG transfer rate.

The thermodynamic parameters describing 12AO and MG12AO dissociation from LFABP were studied by examining the temperature dependence of the rate of 12AO and MG12AO

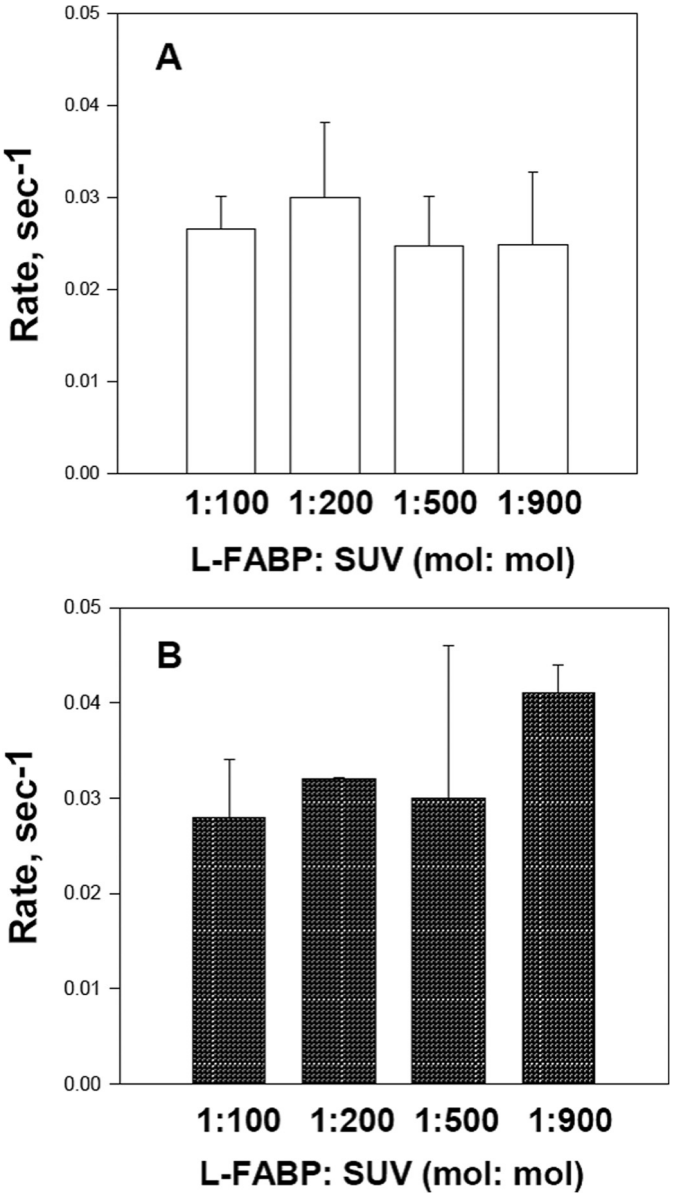

FIGURE 8. **Effect of acceptor vesicle concentration on 12AO (A) or MG12AO (B) transfer from LFABP.** Transfer of 12AO (*A*) or MG12AO (*B*) from LFABP to acceptor EPC SUVs was monitored at 24 °C as described in Fig. 6. Results are means ± S.D. (*error bars*) from five separate experiments.

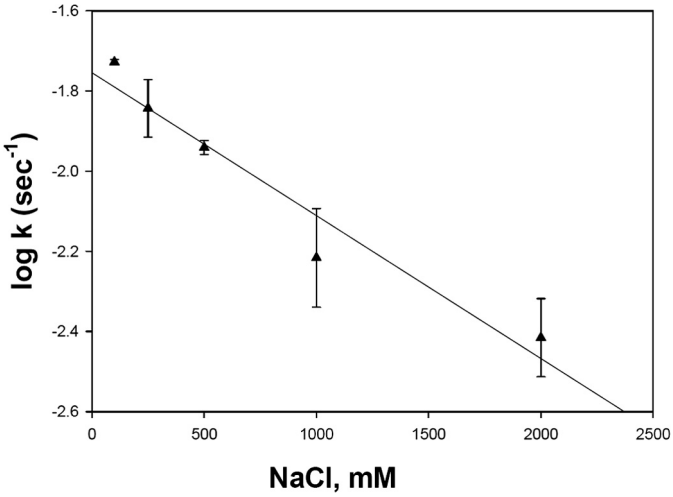

FIGURE 9. **Effect of ionic strength on MG12AO transfer rate from LFABP to EPC SUVs.** The transfer rates and conditions, except for ionic strength, were determined as described in Fig. 6. Results are means ± S.D. (*error bars*) from five separate experiments.

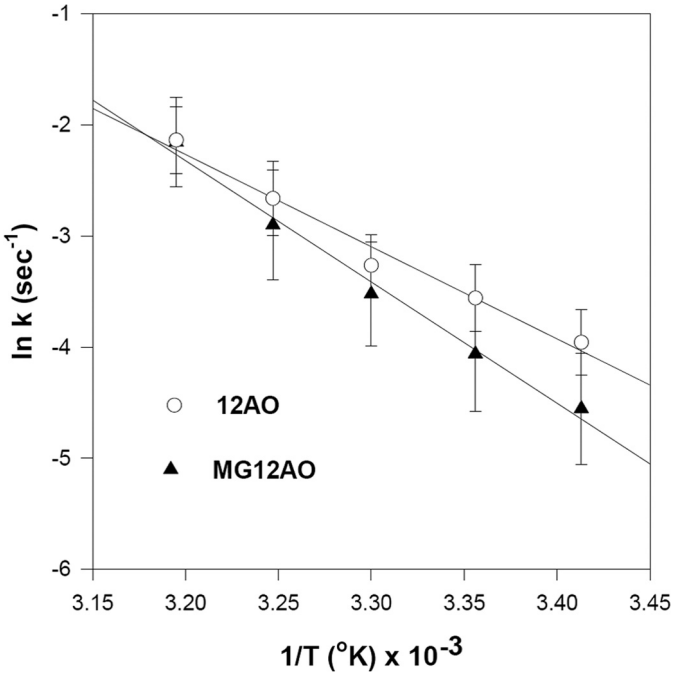

FIGURE 10. **Effect of temperature on 12AO or MG12AO transfer from LFABP to SUVs.** Arrhenius plots of 12AO (○) and MG12AO (▲) transfer from LFABP to EPC SUVs are shown. Conditions, except for temperature, were as described in Fig. 6. Results are means ± S.D. (*error bars*) from five separate experiments.

transfer from LFABP to membranes. The results are shown as Arrhenius plots in Fig. 10. The activation energy (E_a), enthalpy ($\Delta H^{\ddagger}$), entropy ($\Delta S^{\ddagger}$), and Gibbs free energy ($\Delta G^{\ddagger}$) for the transfer process at 25 °C were estimated using the Eyring rate theory (42) and are presented in Table 2. The results show that the free energies of transfer of both 12AO and MG12AO from LFABP to EPC SUVs are very similar and are composed of a decrease in entropy as well as a large enthalpic component, both typical of the aqueous solvation of hydrophobic compounds.

Transfer of 12AO and MG12AO from LFABP to EPC SUVs was further examined as a function of pH. As described previously, the rate of 12AO transfer from LFABP to membranes increased 3–5-fold as pH increased, suggesting that ionization of the FA carboxyl group is an important determinant of the transfer process (40, 43). In contrast, the relative lack of effect of pH on MG12AO transfer rates from LFABP (Fig. 11) presumably reflects the absence of an ionizable functional group in MG12AO.

TABLE 2

Thermodynamic parameters for the transfer of MG12AO and 12AO from LFABP to SUVs

From the rate constants over a temperature range of 15–40 °C, the activation energy was obtained. $\Delta G^{\ddagger}$, $\Delta H^{\ddagger}$, and $\Delta S^{\ddagger}$ of the activated state were estimated at 25 °C as described in the text. Results are in kcal/mol and are means ± S.D. from five separate experiments.

	E_a	$\Delta H^{\ddagger}$	$T\Delta S^{\ddagger}$	$\Delta G^{\ddagger}$
12AO	15.2 ± 2.3	14.6 ± 2.3	−4.9 ± 2.4	19.6 ± 0.2
MG12AO	20.2 ± 1.8	19.6 ± 1.8	−0.3 ± 1.8	19.8 ± 0.3

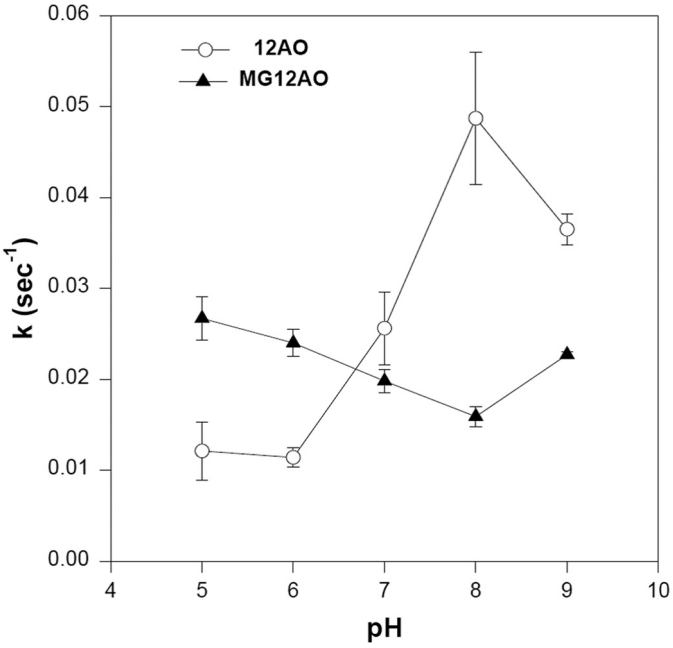

FIGURE 11. **Effect of pH on 12AO (○) and MG12AO (▲) transfer rate from LFABP to SUVs.** Concentrated EPC SUVs and LFABP were diluted into acetate-buffered saline at pH 5 or Tris-buffered saline from pH 6 to 9 prior to assay. Transfer was measured as described in Fig. 6. Results are means ± S.D. (*error bars*) from five separate experiments.

DISCUSSION

We recently showed that intestinal monoacylglycerol metabolism was perturbed in the LFABP-null mouse with less MG incorporated into TG and more used for phospholipid biosynthesis. Because no concomitant changes in the expression of relevant lipid synthesis genes were found, we hypothesized that LFABP plays a role in trafficking of MG toward sites of TG synthesis (14). Nevertheless, there are conflicting reports of monoacylglycerol binding by LFABP (15, 16). Thus, we undertook to determine whether LFABP would bind monoacylglycerol in a physiological context by comparing MG binding in cytosol prepared from wild type and LFABP$^{-/-}$ mouse liver. As demonstrated by Martin *et al.* (22), we confirmed that labeled fatty acid binding in wild type liver cytosol comprises of two distinct compartments: a high molecular mass region at ~66 kDa and a low molecular mass region at ~14 kDa. Because in the present experiments we first perfused the livers to remove blood, the remaining albumin was likely at low levels; therefore, the higher molecular weight peak was not substantial. Immunoblotting showed the presence of LFABP in the low molecular mass ~14-kDa fractions, confirming that LFABP is binding fatty acids in liver cytosol (22). Notably, identical results were obtained using radiolabeled MG with the 14-kDa protein-containing fractions from WT but not LFABP$^{-/-}$ liver cytosol retaining the [^{3}H]monoolein. These results provide strong evidence not only that LFABP does in fact bind MG but also that it does so *in vivo* and is likely to be the major intracellular monoacylglycerol-binding protein in the liver, intestine, and perhaps kidney where LFABP is also expressed.

In contrast to the stoichiometric binding of FA by other FABPs, LFABP binds two FAs (38, 43, 44). Furthermore, whereas other members of the FABP family appear to display high affinity binding only for long chain FAs, LFABP has been shown to bind a number of other small hydrophobic ligands including lysophospholipids (45), heme (46), and bile salts (15, 47). Equilibrium binding analysis using the Lipidex assay indicates that the LFABP binding affinities for FA and MG are in a similar range albeit with MG binding affinity ~2-fold lower than FA binding affinity. Previously, we reported the solution structure of rat liver LFABP, confirming the 2:1 FA:protein stoichiometry and demonstrating for the first time the structural differences in the apo and holo forms of the protein (18). In the present studies, we provide evidence indicating that the solution structure of LFABP with bound monoolein resembles that of the FA-liganded protein with 2 molecules of MG likely to bind in similar positions to the two FA molecules. A definitive structural determination of the MG-protein complex would require intermolecular distance constraints in addition to chemical shift perturbations (48), but the concordance of MG- and OA-affected residues is explained most straightforwardly by similarity of their respective protein-ligand three-dimensional structures.

It is notable that many sites are affected principally either at the early titration stages (0.6–0.8 eq of MG) or else later (1.0–1.2 eq of MG). The location and stepwise pattern of these perturbations parallel our prior investigations of the OA-LFABP binding process in which the first ligand was found to bind deeply within the cavity and the second ligand subsequently bound closer to the aqueous interface (18). However, the fact that most of the perturbed backbone sites exhibit protein heteronuclear single quantum correlation resonances in intermediate exchange ($k \sim \Delta\delta$) during the MG-LFABP titration suggests that apo-single-holo exchange is more facile than in the case of the slowly exchanging OA-FABP, arguing for weaker LFABP interactions with the monoglyceride ligand in keeping with the equilibrium binding analysis.

Having established clearly the binding of MG by LFABP *in vivo* and *in vitro*, we sought to investigate whether LFABP could serve as an intracellular transport protein for MG. Thus, we determined the rate and mechanism of MG transfer from LFABP to membranes in comparison with results for FA transfer and further compared MG transfer from LFABP with MG transfer from membranes. These studies used an AO-labeled monoolein (MG12AO) and the equivalent AO-labeled oleic acid (12AO), both of which we have used previously to examine FA and MG transfer from FABPs, membranes, and micelles (20, 34, 40).

In agreement with our previous results, the transfer rate of the fatty acid analog 12AO from LFABP to membranes increased 3–5-fold as pH increased, suggesting that ionization of the FA carboxyl group is an important determinant of the transfer process (40, 43). In contrast, the relative lack of effect of pH on the monoacylglycerol analog MG12AO transfer rates from LFABP presumably reflects the absence of an ionizable functional group on MG12AO. The similar blue-shifted emission maxima for MG12AO and 12AO in LFABP suggest a similar degree of steric hindrance of the AO fluorophore in the binding site, and the similar fluorescence quantum yields for MG12AO and 12AO bound to LFABP indicate that both lipid probes experience similar noncovalent interactions in a simi-

larly hydrophobic environment upon binding to LFABP. Thus, it is likely that MG binds to LFABP with the glycerol moiety near the protein surface in some degree of contact with the aqueous phase and as supported by the location of the NMR chemical shift perturbations. These binding properties may reflect the ability of LFABP to bind other ligands with bulky head groups, such as lysophosphatidylcholine, as well (45).

The present studies clearly demonstrate that the mechanism of MG12AO transfer from LFABP to SUVs involves aqueous diffusion of the lipid from protein to membrane. Upon increasing the concentration of acceptor membrane, no increase in the transfer rate of MG12AO was observed. This invariance of transfer rate to acceptor is a hallmark of an aqueous diffusion transfer mechanism for hydrophobic compounds (49, 50). We also found that increasing the NaCl concentration of the buffer reduced the rate of MG12AO transfer from LFABP logarithmically, suggesting that the solvation properties of the surrounding aqueous phase regulate the movement of MG from LFABP to membranes. The thermodynamic potentials describing the transfer process were similar for MG12AO and 12AO with nearly identical ΔG values, suggesting that a similar activated state is formed in the transfer of FA and MG from LFABP to the aqueous phase. Therefore, as found previously for FA, the rate-limiting step in the transfer process is likely the dissociation of MG12AO from the donor LFABP into the aqueous phase.

In the absorptive enterocyte, both MG and FA are metabolized in the endoplasmic reticulum with subsequent formation of TG. Large quantities of both metabolites must therefore be transported from their sites of entry across the plasma membrane to their subcellular sites of metabolic utilization. In agreement with our previous report (20), the spontaneous movement of the MG from membrane to membrane is considerably slower than that of the unesterified fatty acid. In distinct contrast, the present results show that transfer of FA and MG derivatives from LFABP to membranes occurs at virtually identical rates. Whereas the absolute transfer rate for 12AO from SUVs or from LFABP is approximately equivalent, the rate of MG12AO transfer is 7-fold faster from LFABP to membranes than from membrane to membrane. It is therefore likely that a function of LFABP may be to facilitate efficient intracellular movement of both major dietary lipid hydrolytic products to their sites of utilization. Although the relative amounts of apo- and holo-LFABP in the enterocyte are not known, the very high level of expression of LFABP in the small intestine (51) suggests it is able to accommodate the binding of FA and MG.

In summary, the present studies demonstrate that LFABP binds monoacylglycerols *in vitro* and *in vivo*. Furthermore, the results show that the MG transfer rate from LFABP is accelerated markedly relative to transfer from membranes. Unlike the slower rate (relative to FA) of MG transfer from membranes, the rates of transfer from LFABP for both these products of dietary TG digestion to acceptor membranes were essentially identical, and transfer of both lipids occurs by an aqueous diffusion mechanism. The similarities in transfer properties are likely to reflect the similar environments experienced by the two ligands when bound to LFABP as verified by the NMR chemical shift perturbation of specific protein sites upon MG ligation. Thus, the results imply that LFABP contributes to the efficient utilization of fatty acids and MG in intestinal TG biosynthesis.

Because LFABP is expressed at high concentrations only in intestine and liver, it remains to be determined which protein(s) binds MG in other cell types that also experience high rates of TG synthesis and lipolysis and may therefore generate significant amounts of MG, such as the adipocyte. As noted above, IFABP was found not to bind MG (16), and we observed no alterations in intestinal MG metabolism in the IFABP$^{-/-}$ mouse in contrast to what was observed in the LFABP$^{-/-}$ mouse (14). To our knowledge, no studies have addressed whether MG is bound by the adipocyte FABP, FABP4, or other members of the FABP family of proteins. Interestingly, it was recently reported that multiple FABPs may bind *N*-acylethanolamines, in particular the arachidonyl derivative *N*-arachidonylethanolamine which, like 2-arachidonoylglycerol, is an endocannabinoid (52). Studies that address the binding of MG in adipose and other tissues are underway.

REFERENCES

1. Phan, C. T., and Tso, P. (2001) Intestinal lipid absorption and transport. *Front. Biosci.* **6,** D299–319
2. Tso, P., and Crissinger, K. (2006) in *Biochemical and Physiological Aspects of Human Nutrition* (Stipanuk, M. H., ed) 2nd Ed., pp. 125–141, W. B. Saunders Co., Philadelphia
3. Maccarrone, M., Gasperi, V., Catani, M. V., Diep, T. A., Dainese, E., Hansen, H. S., and Avigliano, L. (2010) The endocannabinoid system and its relevance for nutrition. *Annu. Rev. Nutr.* **30,** 423–440
4. Di Marzo, V., Bifulco, M., and De Petrocellis, L. (2004) The endocannabinoid system and its therapeutic exploitation. *Nat. Rev. Drug Discov.* **3,** 771–784
5. DiPatrizio, N. V., Astarita, G., Schwartz, G., Li, X., and Piomelli, D. (2011) Endocannabinoid signal in the gut controls dietary fat intake. *Proc. Natl. Acad. Sci. U.S.A.* **108,** 12904–12908
6. Izzo, A. A., Piscitelli, F., Capasso, R., Aviello, G., Romano, B., Borrelli, F., Petrosino, S., and Di Marzo, V. (2009) Peripheral endocannabinoid dysregulation in obesity: relation to intestinal motility and energy processing induced by food deprivation and re-feeding. *Br. J. Pharmacol.* **158,** 451–461
7. Storr, M. A., and Sharkey, K. A. (2007) The endocannabinoid system and gut-brain signalling. *Curr. Opin. Pharmacol.* **7,** 575–582
8. Hansen, K. B., Rosenkilde, M. M., Knop, F. K., Wellner, N., Diep, T. A., Rehfeld, J. F., Andersen, U. B., Holst, J. J., and Hansen, H. S. (2011) 2-Oleoyl glycerol is a GPR119 agonist and signals GLP-1 release in humans. *J. Clin. Endocrinol. Metab.* **96,** E1409–E1417
9. Chon, S. H., Douglass, J. D., Zhou, Y. X., Malik, N., Dixon, J. L., Brinker, A., Quadro, L., and Storch, J. (2012) Over-expression of monoacylglycerol lipase (MGL) in small intestine alters endocannabinoid levels and whole body energy balance, resulting in obesity. *PLoS One* **7,** e43962
10. Ho, S. Y., and Storch, J. (2001) Common mechanisms of monoacylglycerol and fatty acid uptake by human intestinal Caco-2 cells. *Am. J. Physiol. Cell Physiol.* **281,** C1106–C1117
11. Murota, K., and Storch, J. (2005) Uptake of micellar long-chain fatty acid and sn-2-monoacylglycerol into human intestinal Caco-2 cells exhibits characteristics of protein-mediated transport. *J. Nutr.* **135,** 1626–1630
12. Storch, J., and Thumser, A. E. (2000) The fatty acid transport function of fatty acid-binding proteins. *Biochim. Biophys. Acta* **1486,** 28–44
13. Storch, J., and Corsico, B. (2008) The emerging functions and mechanisms of mammalian fatty acid-binding proteins. *Annu. Rev. Nutr.* **28,** 73–95
14. Lagakos, W. S., Gajda, A. M., Agellon, L., Binas, B., Choi, V., Mandap, B., Russnak, T., Zhou, Y. X., and Storch, J. (2011) Different functions of intestinal and liver-type fatty acid-binding proteins in intestine and in whole body energy homeostasis. *Am. J. Physiol. Gastrointest. Liver Physiol.* **300,** G803–G814
15. Thumser, A. E., and Wilton, D. C. (1996) The binding of cholesterol and

bile salts to recombinant rat liver fatty acid-binding protein. *Biochem. J.* **320,** 729–733
16. Storch, J. (1993) Diversity of fatty acid-binding protein structure and function: studies with fluorescent ligands. *Mol. Cell. Biochem.* **123,** 45–53
17. Thumser, A. E., and Storch, J. (2000) Liver and intestinal fatty acid-binding proteins obtain fatty acids from phospholipid membranes by different mechanisms. *J. Lipid Res.* **41,** 647–656
18. He, Y., Yang, X., Wang, H., Estephan, R., Francis, F., Kodukula, S., Storch, J., and Stark, R. E. (2007) Solution-state molecular structure of apo and oleate-liganded liver fatty acid-binding protein. *Biochemistry* **46,** 12543–12556
19. Francis, F. (2007) *Solution-State NMR Studies of Fatty Acid Binding Proteins (FABs)*. Ph.D. dissertation, City University of New York, New York
20. Narayanan, V. S., and Storch, J. (1996) Fatty acid transfer in taurodeoxycholate mixed micelles. *Biochemistry* **35,** 7466–7473
21. Bradford, M. M. (1976) A rapid and sensitive method for the quantitation of microgram quantities of protein utilizing the principle of protein-dye binding. *Anal. Biochem.* **72,** 248–254
22. Martin, G. G., Danneberg, H., Kumar, L. S., Atshaves, B. P., Erol, E., Bader, M., Schroeder, F., and Binas, B. (2003) Decreased liver fatty acid binding capacity and altered liver lipid distribution in mice lacking the liver fatty acid-binding protein gene. *J. Biol. Chem.* **278,** 21429–21438
23. Glatz, J. F., and Veerkamp, J. H. (1983) A radiochemical procedure for the assay of fatty acid binding by proteins. *Anal. Biochem.* **132,** 89–95
24. He, Y., Estephan, R., Yang, X., Vela, A., Wang, H., Bernard, C., and Stark, R. E. (2011) A nuclear magnetic resonance-based structural rationale for contrasting stoichiometry and ligand binding site(s) in fatty acid-binding proteins. *Biochemistry* **50,** 1283–1295
25. Kay, L. E., Keifer, P., and Saarinen, T. (1992) Pure absorption gradient enhanced heteronuclear single quantum correlation spectroscopy with improved sensitivity. *J. Am. Chem. Soc.* **114,** 10663–10665
26. Wishart, D. S., and Sykes, B. D. (1994) The ^{13}C chemical-shift index: a simple method for the identification of protein secondary structure using ^{13}C chemical-shift data. *J. Biomol. NMR* **4,** 171–180
27. Delaglio, F., Grzesiek, S., Vuister, G. W., Zhu, G., Pfeifer, J., and Bax, A. (1995) NMRPipe: a multidimensional spectral processing system based on UNIX pipes. *J. Biomol. NMR* **6,** 277–293
28. Johnson, B. A., and Blevins, R. A. (1994) NMR View: a computer program for the visualization and analysis of NMR data. *J. Biomol. NMR* **4,** 603–614
29. Mulder, F. A., Schipper, D., Bott, R., and Boelens, R. (1999) Altered flexibility in the substrate-binding site of related native and engineered high-alkaline *Bacillus* subtilisins. *J. Mol. Biol.* **292,** 111–123
30. Huang, C., and Thompson, T. E. (1974) Preparation of homogeneous, single-walled phosphatidylcholine vesicles. *Methods Enzymol.* **32,** 485–489
31. Gomori, G. (1942) A modification of the colorimetric phosphorus determination for use with the photoelectric colorimeter. *J. Lab. Clin. Med.* **27,** 955–960
32. Parker, C. A., and Rees, W. T. (1960) Correction of fluorescence spectra and measurement of fluorescence quantum efficiency. *Analyst* **85,** 587–600
33. Scott, T. G., Spencer, R. D., Leonard, N. J., and Weber, G. (1970) Emission properties of NADH. Studies of fluorescence lifetimes and quantum efficiencies of NADH, AcPyADH, and simplified synthetic models. *J. Am. Chem. Soc.* **92,** 687–695
34. Storch, J., and Kleinfeld, A. M. (1986) Transfer of long-chain fluorescent free fatty acids between unilamellar vesicles. *Biochemistry* **25,** 1717–1726
35. Storch, J., and Bass, N. M. (1990) Transfer of fluorescent fatty acids from liver and heart fatty acid-binding proteins to model membranes. *J. Biol. Chem.* **265,** 7827–7831
36. Wootan, M. G., Bernlohr, D. A., and Storch, J. (1993) Mechanism of fluorescent fatty acid transfer from adipocyte fatty acid binding protein to membranes. *Biochemistry* **32,** 8622–8627
37. Wang, H., He, Y., Kroenke, C. D., Kodukula, S., Storch, J., Palmer, A. G., and Stark, R. E. (2002) Titration and exchange studies of liver fatty acid-binding protein with ^{13}C-labeled long-chain fatty acids. *Biochemistry* **41,** 5453–5461
38. Thompson, J., Winter, N., Terwey, D., Bratt, J., and Banaszak, L. (1997) The crystal structure of the liver fatty acid-binding protein. A complex with two bound oleates. *J. Biol. Chem.* **272,** 7140–7150
39. Matayoshi, E. D., and Kleinfeld, A. M. (1981) Emission wavelength-dependent decay of the 9-anthroyloxy-fatty acid membrane probes. *Biophys. J.* **35,** 215–235
40. Kim, H. K., and Storch, J. (1992) Free fatty acid transfer from rat liver fatty acid-binding protein to phospholipid vesicles. Effect of ligand and solution properties. *J. Biol. Chem.* **267,** 77–82
41. Hsu, K. T., and Storch, J. (1996) Fatty acid transfer from liver and intestinal fatty acid-binding proteins to membranes occurs by different mechanisms. *J. Biol. Chem.* **271,** 13317–13323
42. Glasstone, S., Laidler, K., and Eyring, E. (1941) *The Theory of Rate Processes*, McGraw-Hill, New York
43. Cistola, D. P., Walsh, M. T., Corey, R. P., Hamilton, J. A., and Brecher, P. (1988) Interactions of oleic acid with liver fatty acid binding protein: a carbon-13 NMR study. *Biochemistry* **27,** 711–717
44. Keuper, H. J., Klein, R. A., and Spener, F. (1985) Spectroscopic investigations on the binding site of bovine hepatic fatty acid binding protein. Evidence for the existence of a single binding site for two fatty acid molecules. *Chem. Phys. Lipids* **38,** 159–173
45. Thumser, A. E., Voysey, J. E., and Wilton, D. C. (1994) The binding of lysophospholipids to rat liver fatty acid-binding protein and albumin. *Biochem. J.* **301,** 801–806
46. Epstein, L. F., Bass, N. M., Iwahara, S., Wilton, D. C., and Muller-Eberhard, U. (1994) Immunological identity of rat liver cytosolic heme-binding protein with purified and recombinant liver fatty acid binding protein by Western blots of two-dimensional gels. *Biochem. Biophys. Res. Commun.* **204,** 163–168
47. Fujita, M., Fujii, H., Kanda, T., Sato, E., Hatakeyama, K., and Ono, T. (1995) Molecular cloning, expression, and characterization of a human intestinal 15-kDa protein. *Eur. J. Biochem.* **233,** 406–413
48. Guan, X. (2011) *Biophysical Studies of Molecular Recognition in Peripheral and Integral Membrane Proteins*. Ph.D. dissertation, The City University and The City College of New York, New York
49. Brown, R. E. (1992) Spontaneous lipid transfer between organized lipid assemblies. *Biochim. Biophys. Acta* **1113,** 375–389
50. Roseman, M. A., and Thompson, T. E. (1980) Mechanism of the spontaneous transfer of phospholipids between bilayers. *Biochemistry* **19,** 439–444
51. Ockner, R. K. (1990) Historic overview of studies on fatty acid-binding proteins. *Mol. Cell. Biochem.* **98,** 3–9
52. Kaczocha, M., Glaser, S. T., and Deutsch, D. G. (2009) Identification of intracellular carriers for the endocannabinoid anandamide. *Proc. Natl. Acad. Sci. U.S.A.* **106,** 6375–6380

Liver Fatty Acid-binding Protein Binds Monoacylglycerol *in Vitro* and in Mouse Liver Cytosol

William S. Lagakos, Xudong Guan, Shiu-Ying Ho, Luciana Rodriguez Sawicki, Betina Corsico, Sarala Kodukula, Kaeko Murota, Ruth E. Stark and Judith Storch

J. Biol. Chem. 2013, 288:19805-19815.
doi: 10.1074/jbc.M113.473579 originally published online May 8, 2013